Spectral phase retrieval of 8 fs optical pulses at 600 nm by using a collinear autocorrelator with 300-μm-thick lithium triborate crystals

Chen-Shao Hsu,[1] Yu-Hsien Lee,[2] Atsushi Yabushita,[2] Takayoshi Kobayashi,[2,3,4,5] and Shang-Da Yang[1,*]

[1]*Institute of Photonics Technologies, National Tsing Hua University, Hsinchu 30013, Taiwan*

[2]*Department of Electrophysics, National Chiao-Tung University, Hsinchu 30013, Taiwan*

[3]*Department of Engineering Science, Advanced Ultrafast Laser Research Center, University of Electro-Communications, Chofugaoka 1-5-1, Chofu, Tokyo 182-8585, Japan*

[4]*International Cooperative Research Project (ICORP), Japan Science and Technology Agency (JST), 4-1-8 Honcho, Hawaguchi, Saitama 332-0012, Japan*

[5]*Institute of Laser Engineering, Osaka University, 2-6 Yamada-oka, Suita, Osaka 565-0971, Japan*

**Corresponding author: shangda@ee.nthu.edu.tw*

Received March 9, 2011; revised April 27, 2011; accepted April 27, 2011; posted April 28, 2011 (Doc. ID 143885); published May 26, 2011

We report on noniterative spectral phase retrieval of 1.1 nJ, 8 fs pulses at 600 nm by using 300-μm-thick lithium triborate crystals in a standard collinear autocorrelator with ≈2 min data acquisition time. This method is simple, sensitive, and immune to the spectral distortion and UV absorption of the linear and nonlinear optics. © 2011 Optical Society of America

OCIS codes: 320.7100, 320.7110.

Few- and single-cycle optical pulses have been widely applied to time-resolved spectroscopy [1] and generation of isolated attosecond pulses [2], where the spectral phases of these ultrabroadband pulses are crucial for the time resolution and emitted photon energy, respectively. Measurement of sub-10 fs optical pulses have been demonstrated by a few methods. Frequency-resolved optical gating (FROG) of multishot [3] and single-shot [4] configurations successfully characterized 4–5 fs pulses at 800 nm, where extremely thin (10 and 5 μm) beta barium borate (BBO) crystals with blueshifted central phase-matching wavelengths (350 and 262 nm) were used to cover the entire second-harmonic bandwidth. However, they have low measurement sensitivity (requiring 15 nJ and 10 μJ) and need to correct the uneven spectral responses of the BBO, optical components, and CCD over a wide bandwidth. Additional errors could arise from the geometrical time smearing in a multishot scheme, as well as the low conversion and detection efficiencies around the short-wavelength spectral wing in both schemes [3,4]. Measurement of ≈6 fs pulses by spectral phase interferometry for direct electric-field reconstruction (SPIDER) was also demonstrated [5]. It is single-shot, noniterative and can use a thicker (30 μm) BBO crystal due to the larger tolerance of phase-matching bandwidth. Nevertheless, SPIDER requires (1) demanding precision of delay calibration (≈10 as) when measuring single-cycle pulses [6], (2) stringent spectral resolution of the spectrometer, and (3) the chirped pulse duration and the delay between the two signal pulse replicas have to be simultaneously adjusted to measure different pulses.

Two variations of SPIDER were proposed to mitigate the above problems and successfully measured sub-10 fs pulses. In the spatially encoded arrangement (SEA) SPIDER experiment [7], the two spectrally sheared pulses were crossed at an angle to encode the spectral phase information of the 8.6 fs pulse in the spatial fringes. This method solves for the last two problems and has high sensitivity (3.8 nJ) and high dynamic range (20 dB). However, SEA SPIDER needs to select two out of the five upconverted beams and have them properly interfered on a 2D camera, which is complicated and may cause delay calibration issues in the presence of imaging aberrations or misalignments [8]. Two-dimensional spectral shearing interferometry (2DSI) [8,9] encodes the spectral phase information of ≈5 fs pulses in the temporal fringes by scanning the relative phase between the two quasi-CW beams. It is immune to all the three problems, but still needs spectral shear calibration. Note that SPIDER and its variants used 30-μm-thick type-II BBO crystals, where the phase-matching curve has octave-spanning bandwidths in one polarization and narrow bandwidths in the other when measuring pulses centered at 800 nm [9]. This fortuitous coincidence, however, does not apply to other wavelengths.

We have demonstrated direct complex field retrieval of ≈400 fs pulses by a modified interferometric field autocorrelation (MIFA) method using a standard collinear autocorrelator, a thick nonlinear crystal, and a slow point detector [10,11]. In addition to the greatly simplified and cost-effective setup, the employment of thick nonlinear crystals makes MIFA particularly attractive in measuring few-cycle pulses because of (1) high second-harmonic generation (SHG) efficiency and measurement sensitivity, and (2) immunity to the spectral distortion caused by the linear and nonlinear optics. Since the MIFA trace itself encodes the central phase-matching wavelength of the crystal, the system is free of any critical calibration and applicable to a wide variety of different pulses. As a proof of concept, we used two 300-μm-thick type-I lithium triborate (LBO) crystals in a MIFA setup to retrieve the spectral phase of an 8 fs signal pulse centered at 600 nm (corresponding to four optical cycles) at 1.1 nJ pulse energy. The measurement result is consistent with

an independent FROG measurement using 10-μm-thick type-I BBO crystal at 28 nJ.

As explained in [10,11], processing the interferometric autocorrelation trace due to a thick nonlinear crystal (i.e. the MIFA trace) with central phase-matching frequency $2f_0$ gives an "even" spectral phase function $\psi_{e1}(f) = [\psi(f) + \psi(-f)]/2$, where $\psi(f)$ is the phase of the complex spectral envelope $A(f)$ of the unknown pulse with carrier frequency f_0. By taking a second MIFA trace with a shifted central phase-matching frequency of $2(f_0 - \Delta)$, one can retrieve another spectral phase function $\psi_{e2}(f) = [\psi(f) + \psi(-f - 2\Delta)]/2$. A recursive formula can be used to reconstruct the complete $\psi(f)$ function:

$$\psi(f - 2\Delta) - \psi(f) = 2[\psi_{e2}(f - 2\Delta) - \psi_{e1}(f)]. \quad (1)$$

Figure 1 shows our experimental setup, consisting of a collinear Michelson interferometer (MI), two 300-μm-thick LBO crystals, and a spectrometer (USB2000+, Ocean optics). The 5 kHz, 8 fs (90 THz bandwidth), 600 nm signal pulse train came from a noncollinear optical parametric amplifier (NOPA) as used in [1]. The MI used an electrically controlled stage (FS-1020PX, Sigma Tech) to scan the optical path with a step size of 120 nm. In every step, the controller would feed back the stage position (delay value) with 10 nm (66 as) accuracy. The signal pulse pair was coupled into two 300-μm-thick LBO crystals by a curved mirror with 4 in focal length for SHG. The two crystals were oriented differently such that the corresponding central phase-matching wavelengths were 314.2 and 320.6 nm ($f_0 =$ 477.4 THz, $\Delta = 9.5$ THz), respectively (Fig. 2). The average SH powers at the two wavelengths were simultaneously recorded by a spectrometer with 50 ms integration time as a function of delay. It took ≈2 min to acquire two MIFA traces of an 80 fs delay window. One can also use one LBO crystal and a GaP point detector (no spectrometer) to acquire two MIFA traces in two sequential steps. We utilized the parallel mode in an attempt to shorten the data acquisition time and suppress the error due to the fluctuation of the signal pulse train.

The crystal thickness has a profound impact on the accuracy of the experiment. First, the crystal has to be thick enough such that the phase-matching bandwidth is much narrower than that of the nonlinear polarization spectrum (a prerequisite of the MIFA method). Second, the crystal should be thin enough to prevent the fundamental pulse from serious broadening due to group velocity dispersion (GVD). Figure 2 illustrates the nonlinear polarization power spectrum (shaded curve) obtained by assuming the experimentally measured spectral intensity

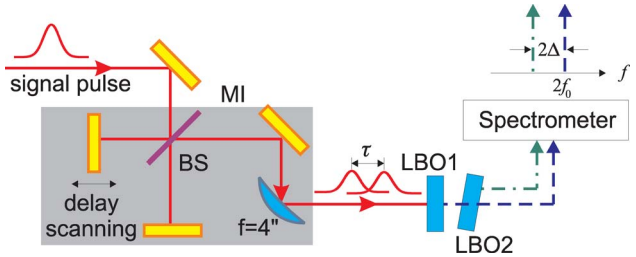

Fig. 1. (Color online) Experimental setup. BS, pellicle beam splitter; MI, Michelson interferometer.

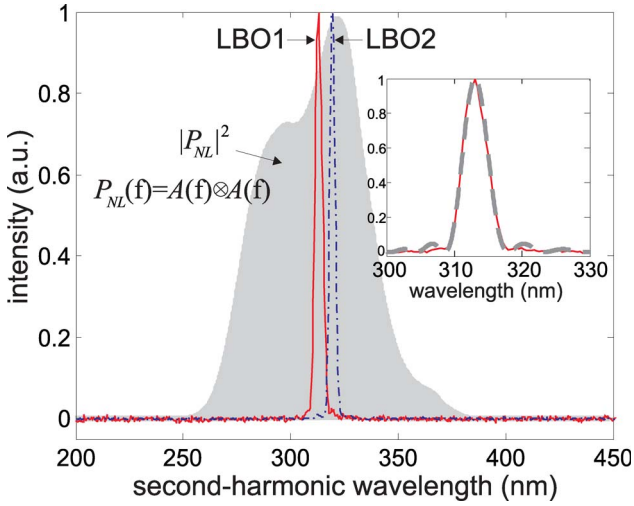

Fig. 2. (Color online) Nonlinear polarization power spectrum (shaded curve) obtained by assuming the experimentally measured spectral intensity and constant spectral phase. Experimentally measured second-harmonic power spectra due to the two 300-μm-thick LBO crystals (solid, dashed-dotted curves), respectively. Inset, measured (solid curve) and simulated (dashed curve) phase-matching power spectra of LBO1.

(Fig. 4, dashed curve) and constant spectral phase, as well as the second-harmonic (phase-matching) power spectra (solid, dashed-dotted curves) due to the two 300-μm-thick LBO crystals, respectively. The inset shows that the measured (solid curve) and simulated (dashed curve) phase-matching power spectra of LBO1 are in good agreement. The two phase-matching peaks of LBO1 and LBO2 are well separated, suppressing the error due to recursive reconstruction. Each has a bandwidth (FHWM) of 3.7 nm (11.9 THz), about 13% of the signal bandwidth (90 THz). The narrow second-harmonic signal bandwidth eliminates the requirement of spectral correction for linear and nonlinear optics. Furthermore, the complete spectral phase can still be retrieved even though both phase-matching peaks are deviated from the spectral center of the nonlinear polarization [12].

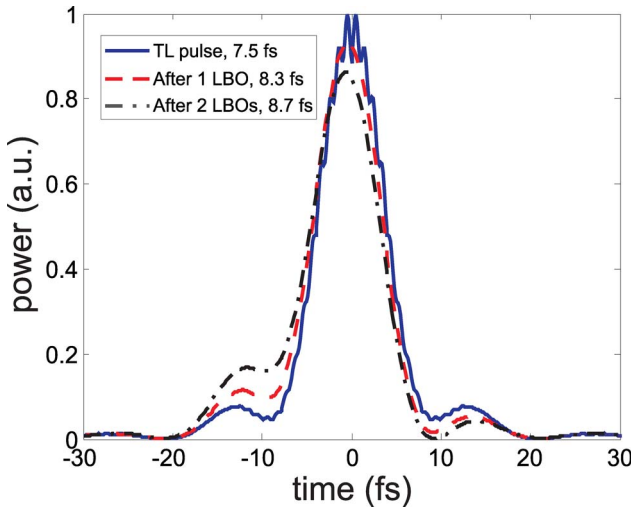

Fig. 3. (Color online) Simulated temporal intensity profiles of the transform-limited pulse (solid curve) and the dispersed pulses after passing through one (dashed curve) and two (dashed-dotted curve) LBO crystals, respectively.

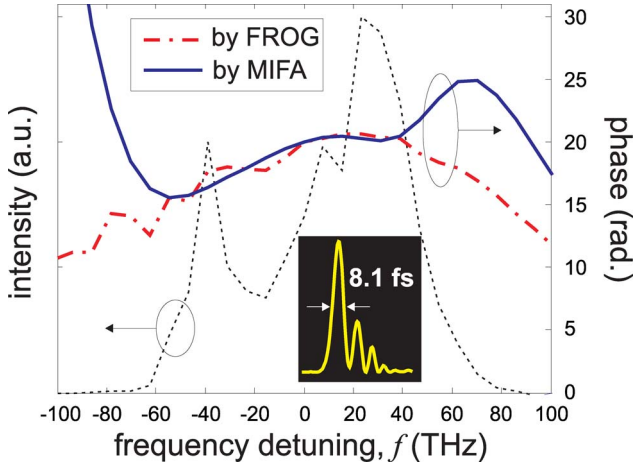

Fig. 4. (Color online) The power spectrum measured by a spectrometer (dashed curve), and the spectral phases retrieved by FROG (dashed-dotted curve) and MIFA (solid curve), respectively. Inset, temporal intensity profile arising from the spectral intensity and phase measured by spectrometer and MIFA, respectively.

These advantages are particularly evident in few-cycle pulse measurement, where expensive UV-enhanced optics and detectors are usually needed and the strong UV absorption of nonlinear crystals is a challenging issue. The GVD effect was analyzed by simulation using the experimentally measured fundamental power spectrum of the NOPA pulse and the Sellmeier equation of LBO [13]. Figure 3 shows the simulated temporal intensity profiles of the transform-limited pulse (solid curve) and the dispersed pulses after passing through one (dashed curve) and two (dashed-dotted curve) LBO crystals, respectively. The corresponding FWHM values are 7.5, 8.3, and 8.7 fs, respectively, indicating that the GVD of 300(600)-μm-thick LBO crystal is not critical in our measurement. By comparison, a 160-μm-thick BBO can achieve the same phase-matching bandwidth (11.9 THz) but will seriously broaden the input pulse to 9.8 and 14.7 fs (double pass), respectively.

Figure 4 illustrates the spectral phase profiles of the signal pulse retrieved by MIFA (solid curve) and FROG (dashed-dotted curve, with a FROG error of 0.015), which are in good agreement over the spectral range where the spectral intensity (dotted curve) remains appreciable. The disagreement at the spectral wings is attributed to the fact that the FROG and MIFA setups used different optical components and were separated by 2.75 m apart (limited by the lab space), which might introduce different dispersions. The temporal intensity arising from the spectral phase retrieved by MIFA and the spectral intensity measured by a spectrometer has an FWHM of 8.1 fs, corresponding to four optical cycles around 600 nm wavelength. Note that the FROG trace was measured by a 10-μm-thick BBO crystal at a minimum coupled pulse energy of 28 nJ (data acquisition time ≈1 min), which is much higher than the 1.1 nJ used in the MIFA measurement. In summary, we have demonstrated that the MIFA method using thick nonlinear crystals can retrieve the spectral phase of 8 fs pulses analytically. This method has a simple, cost-effective setup, high measurement sensitivity, and is immune to the spectral distortion and strong UV absorption of the linear and nonlinear optics. It is applicable to pulses of different durations and central wavelengths without critical recalibration.

This material is supported by the National Science Council of Taiwan (NSCT) under grant NSC 97-2221-E-007-028-MY3, NSC 98-2112-M-009-001-MY3, and NSC 99-2120-M-007-010.

References

1. A. Yabushita, Y. H. Lee, and T. Kobayashi, Rev. Sci. Instrum. **81**, 063110 (2010).
2. F. Krausz and M. Ivanov, Rev. Mod. Phys. **81**, 163 (2009).
3. A. Baltuška, M. S. Pshenichnikov, and D. A. Wiersma, Opt. Lett. **23**, 1474 (1998).
4. S. Akturk, C. D'Amico, and A. Mysyrowicz, J. Opt. Soc. Am. B **25**, A63 (2008).
5. L. Gallmann, D. H. Sutter, N. Matuschek, G. Steinmeyer, U. Keller, C. Iaconis, and I. A. Walmsley, Opt. Lett. **24**, 1314 (1999).
6. J. R. Birge and F. X. Kärtner, J. Opt. Soc. Am. B **25**, A111 (2008).
7. A. S. Wyatt, I. A. Walmsley, G. Stibenz, and G. Steinmeyer, Opt. Lett. **31**, 1914 (2006).
8. J. R. Birge, R. Ell, and F. X. Kärtner, Opt. Lett. **31**, 2063 (2006).
9. J. R. Birge, H. M. Crespo, and F. X. Kärtner, J. Opt. Soc. Am. B **27**, 1165 (2010).
10. S.-D. Yang, C.-S. Hsu, S.-L. Lin, H. Miao, C.-B. Huang, and A. M. Weiner, Opt. Express **16**, 20617 (2008).
11. S.-D. Yang, C.-S. Hsu, S.-L. Lin, Y.-S. Lin, C. Langrock, and M. M. Fejer, Opt. Lett. **34**, 3065 (2009).
12. L. F. Yang, S. L. Lin, and S. D. Yang, Opt. Express **18**, 6877 (2010).
13. D. N. Nikogosyan, *Nonlinear Optical Crystals: A Complete Survey* (Springer, 2005).